

Direct Fabrication of Yttrium Aluminium Garnet Nanofibers by Electrospinning

Khalil Abdelrazek Khalil^{1,2,*}, Abdulhakim A. Almajid¹, Ehab A. El-Danaf¹, Magdy M. El Rayes^{1,4} and El-Sayed M. Sherif³

¹ Mechanical Engineering Department, NPST, King Saud University, P.O. Box 800, Riyadh 11421, Saudi Arabia

² Material Engineering and Design Department, Faculty of Energy Engineering, Aswan University, Aswan, Egypt

³ Center of Excellence for Research in Engineering Materials (CEREM), College of Engineering, King Saud University, P. O. Box 800, Al-Riyadh 11421, Saudi Arabia

⁴ On leave from Production Engineering Department, Faculty of Engineering, Alexandria University, Egypt.

*E-mail: kabdelmawgoud@KSU.EDU.SA

Received: 7 October 2012 / Accepted: 31 October 2012 / Published: 1 December 2012

In this work, the technique of electrospinning has been employed to fabricate uniform one-dimensional (1-D) Yttrium aluminum garnet (YAG) nanofibers. YAG precursor was prepared by sol-gel method using ethanol as solvent. Alcoholic solutions containing polyvinyl Alcohol (PVA) have been used as a gel. The sol-gel was then introduced to the electrospinning apparatus to form nanofibers. Upon firing and sintering under carefully pre-selected time-temperature profiles, ceramic nanofibers retaining the original morphological features observed in the as-spun composition are obtained. Calcination has been done at different temperatures (800, 900, and 1000 °C). Analytical tools, such as TGA and SEM have been employed to elucidate the pathway of ceramic phase formation and the systematic evolution of morphological features in the spun and the processed fibers. X-ray diffraction has also been used to identify the crystalline state of the final products. Pure crystalline YAG phase was obtained at 800 °C, without any intermediate phases such as $YAlO_3$ (YAP) and $Y_4Al_2O_9$ (YAM). The calcination temperature used in this study is significantly lower than that required by the conventional solid-state reaction process and comparable with that required by most of the chemical-based synthesis routes.

Keywords: Electrospinning, Yttrium Aluminium Garnet, Coating, Calcination.

1. INTRODUCTION

Yttrium Aluminum Garnet (YAG, with chemical formula $Y_3Al_5O_{12}$) with a cubic garnet structure has received much attention due to its interesting optical and mechanical properties. It has

emerged as the most widely produced laser gain host and has enjoyed recent popularity as a promising material for optical, electronic and structural applications [1, 2]. YAG is also a candidate for applications of high-temperature structural materials due to its low creep rate and high thermal stability and good chemical resistance [3, 4]. YAG powders were conventionally synthesized by solid-state reaction process using Y_2O_3 and Al_2O_3 as starting materials. The solid-state reaction process usually requires a calcination temperature above 1600 °C [5]. The high calcination temperature inevitably leads to coarsening microstructures and, thus, affects the sinterability of the synthesized powders. In order to reduce the crystallization temperature, improve the phase purity of the final product and reach a highly homogeneous distribution of the two phases in the composite material, several types of wet chemical methods [2, 6–10] have been already developed and successfully used for powder processing. In addition to solid-state reaction [5, 11, 12], there are many other methods of synthesizing YAG powders, such as co-precipitation [13, 14], spray pyrolysis [15], hydrothermal synthesis [16] and sol-gel combustion [17, 18]. Compared with the other methods, the sol-gel method is one of the most promising techniques because of its inexpensive starting materials, simple synthesis process, lower heat-treated temperature and achievement of homogeneous multi component powders. Nowadays, it has attracted more and more attention and been widely used to prepare the pure-phase YAG powders. The solvent used in conventional sol-gel methods was usually deionized water, and pure-phase YAG powders were obtained by rapidly calcining the precursors up to high temperatures (≥ 900 °C) [17–21]. For example, coprecipitation process has reduced the formation temperature of YAG phase to 900–1200 °C [22–24], while formation of YAG can take place at 900 °C for sol-gel process. However, the chemical processes are of some intrinsic disadvantages over the conventional solid-state reaction one. For example, coprecipitation usually uses chloride or nitrate salts. Though the presence of anions can enhance the final product morphology, but at the same time it can damage properties of the synthesized powders. Removing these ions requires repeated washing, which in turn alters the compositions of the precipitates. This makes it difficult to control the stoichiometric composition of the designed compound.

On the other hand, electrospinning, an electrostatic fiber fabrication technique has evinced more interest and attention in recent years due to its versatility and potential for applications in diverse fields [25]. The notable applications include tissue engineering, biosensors, filtration, wound dressings, drug delivery, and enzyme immobilization. The nanoscale fibers are generated by the application of strong electric field on polymer solution or melt. The non-wovens nanofibrous mats produced by this technique could be considered as mimics extracellular matrix components much closely as compared to the conventional techniques. The sub-micron range spun fibers produced by this process, offer various advantages like high surface area to volume ratio, tunable porosity and the ability to manipulate nanofiber composition in order to get desired properties and function [26–28]. Thus far, a number of metal-oxide nanofibers such as ZnO, SnO₂, TiO₂, and BaTiO₃ have been successfully produced in a facile manner by an electrospinning method. During this process, reactions such as hydrolysis, condensation and gelation of the precursors are involved in the morphological evolution of the fibers. Next, the composite nanofibers are calcined at high temperatures, resulting in polycrystalline metal-oxide nanofibers [29, 30].

The main objective of this investigation was the fabrication of Yttrium Aluminum Oxide nanofibers of high phase purity, which has several nanometer diameter and uniform. YAG nanofiber was synthesized by electrospinning of a sol containing ethanol as solvent of YAG precursor and an alcoholic solutions containing polyvinyl Alcohol (PVA) as a gel. By this method, pure crystalline YAG nanofiber phase was obtained at temperature as low as 800 °C. The effects of calcination temperatures on the formation of YAG phase have been mainly discussed.

2. EXPERIMENTAL

Aluminum (III) nitrate nonahydrate ($\text{Al}(\text{NO}_3)_3 \cdot 9\text{H}_2\text{O}$, 99.99%) A.C.S. reagent from SIGMA-ALDRICH, yttrium nitrate hexahydrate ($\text{Y}(\text{NO}_3)_3 \cdot 6\text{H}_2\text{O}$, 99.99%), from ALDRICH, citric acid monohydrate ($\text{C}_6\text{H}_8\text{O}_7 \cdot \text{H}_2\text{O}$, 99.50%) and ethanol were used as starting materials. The molar ratio of $\text{Al}(\text{NO}_3)_3 \cdot 9\text{H}_2\text{O}$ to $\text{Y}(\text{NO}_3)_3 \cdot 5\text{H}_2\text{O}$ was 5: 3. $\text{Al}(\text{NO}_3)_3 \cdot 9\text{H}_2\text{O}$, $\text{Y}(\text{NO}_3)_3 \cdot 5\text{H}_2\text{O}$ and $\text{C}_6\text{H}_8\text{O}_7 \cdot \text{H}_2\text{O}$ were dissolved in ethanol with appropriate stoichiometric amounts. $\text{Y}_3\text{Al}_5\text{O}_{12}$ precursor sol was obtained by refluxing a solution of the above mentioned precursors using magnetic stirring for 6 h at room temperature. Polyvinyl alcohol (PVA) with an average molecular weight of 65,000 /mol and percentage of hydrolysis equal to 98 – 99 has been used as gel solution. Distilled water was used as the solvent. PVA granules were dissolved in distilled water at 70 °C with vigorous stirring for at least 1 hr to prepare 20 ml of 10 wt. % PVA solution. After cooling down the resulting solution were added to the solution of $\text{Y}_3\text{Al}_5\text{O}_{12}$ precursor sol and stirred for additional 1 h.

In this stage, the sol–gel reaction took place within the precursors and a homogeneous viscous solution was obtained. Subsequently, the solution was filled in a 20 mL NORM-JECT Luer Lok tip plastic syringe having an 18 gauge stainless-steel needle with 90° blunt end. The electrospinning setup included high voltage power supply, purchased from the NanoNC, Inc. (S. Korea), and a nanofiber collector of aluminum foil that covered a laboratory produced roller with the diameter of 12 cm. The collector was placed at 20 cm tip to collector distance (TCD). During electrospinning, a positive high voltage of 20 kV was applied to the needle; and the solution feed rate of 0.1 mL/h was maintained using a KDS 200 syringe pump purchased from the KD Scientific Inc. (Holliston, MA). The schematic diagram of electrospinning process is shown in Fig. 1. The electrospun nano-fibrous could be readily peeled off from the aluminum foil, and the obtained nano-fibrous were stored in a desiccator before the subsequent calcination process. The as-prepared aluminum yttrium oxide/PVA composite fibers were collected and calcinated at different temperatures to get pure $\text{Y}_3\text{Al}_5\text{O}_{12}$ fibers with nano to submicron diameters. The thermal degradation behaviors of the nanofiber were studied with a thermogravimetric analyzer (TA Instruments, Q500 TGA, United States); instrument in the temperature range from 20 °C to 800 °C under nitrogen at a flow rate of 40 ml/min and at a heating rate of 10 °C/min. The surface morphology of the nanofiber was observed with SEM (JEOL GSM-6610LV) scanning electron microscope and JEOL GSM-7600F field emission scanning electron microscope at an accelerated voltage of 10 kV. The surfaces were vacuum-coated with platinum for SEM. The structure of the nanofiber was analyzed by *FT-IR* spectra. The fiber sample were measured by sensor (Bruker,

TENSOR Series FT-IR Spectrometer, Germany), connected to a PC, and analysis the data by IR Solution software, analytical methods are standard in *OPUS*TM software.

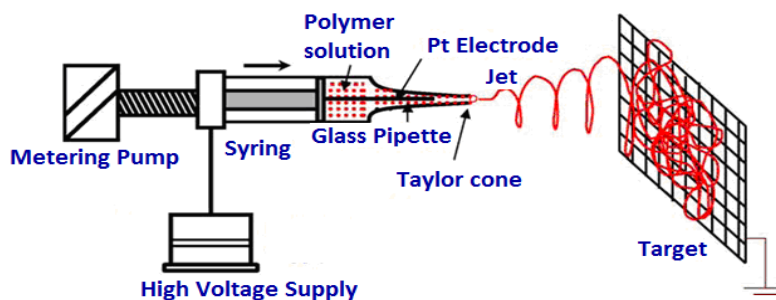


Figure 1. Schematic diagram of electrospinning set up.

The nanofiber precalcined at 500 °C for 3 hrs, and then calcined in air at temperatures of 800, 900 and 1000 °C for 2 hrs, respectively. The calcination profile was done according to the schedule shown in Figure 2. The heating rates were chosen so as to ensure the removal of organic components without destroying the nanofibrillar morphological features in the end products and also to avoid the disintegration of the ceramic fibers; as such, ceramics exhibit rather poor thermal shock resistance, even in bulk. After the furnace was cooled, samples were collected for characterization by various analytical techniques.

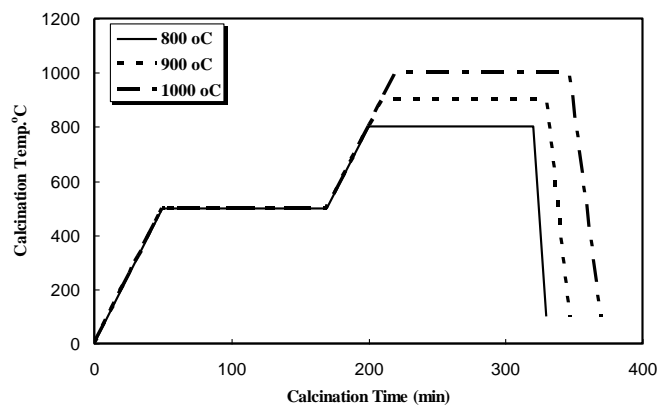


Figure 2. Calcination temperatures for YAG nanofibers

3. RESULTS AND DISCUSSIONS

Syntheses of oxide materials using sol-gel methods which employ soluble polymers have previously been reported [31, 32]. Ternary oxides like $Y_3Fe_5O_{12}$ (YIG) have also been produced via a sol-gel process, in which the organic modification of the starting precursors leads to the formation of sols exhibiting a dynamic viscosity [33]. Fig. 3 shows the scanning electron micrographs of the $Y_3Al_5O_{12}$ -PVA composite fibers collected on the aluminum foil. The electrospinning process produced

relatively smooth nanofibers. Beads or agglomerated nanofibers cannot be observed in the obtained mats. As can be seen in this figure, the solution has produced a smooth morphology for nanofibers with wide ranges of diameters. On the other hand, all fibers exhibited uniform diameters with several micrometers in length. It is also observed that most of the as-spun nanofibers have diameter of about 200 nm and are round and uniform over a length of several micrometers. The energy dispersive spectrum (EDS) collected on the $Y_3Al_5O_{12}$ -PVA sample (whose microstructure is illustrated in Fig. 3) distinctly identifies Y and Al as the elemental component in the fiber and is shown in Fig. 4. The other peaks belonging to carbon are generated from the PVA used to prepare the viscous solution of the sol-gel.

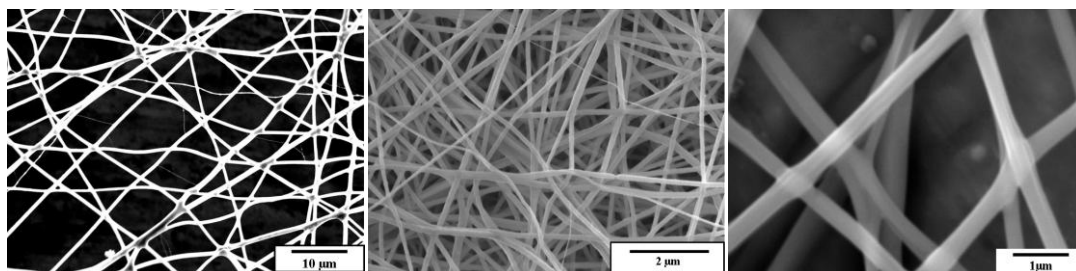


Figure 3. SEM image of $Y_3Al_5O_{12}$ -PVA as-spun nanofibers at different magnifications

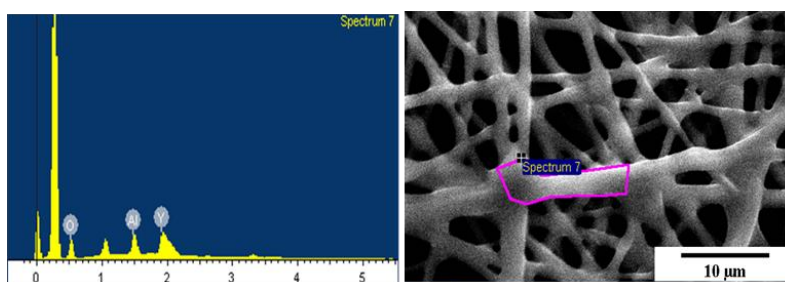


Figure 4. EDX analysis of $Y_3Al_5O_{12}$ -PVA as-spun nanofibers.

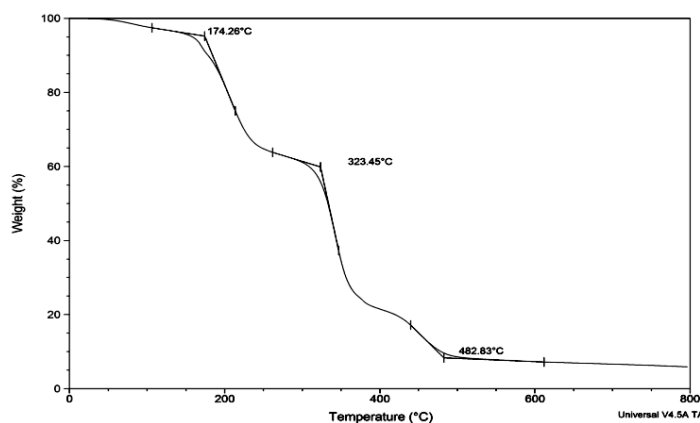


Figure 5. TGA curve of thermal decomposition of the as-spun $Y_3Al_5O_{12}$ /PVA composite nanofibers at a heating rate of 5 °C/min in static air.

Fig. 5 shows the TGA thermal decomposition of the as-spun $Y_3Al_5O_{12}/PVA$ composite nanofibers at a heating rate of $5\text{ }^\circ\text{C}/\text{min}$ in static air. It can be seen that, a minor weight loss step at about $200\text{ }^\circ\text{C}$ and a major weight loss step from $200\text{ }^\circ\text{C}$ up to about $500\text{ }^\circ\text{C}$. No further weight loss was observed up to $800\text{ }^\circ\text{C}$. The minor weight loss was related to the loss of moisture and trapped solvent (water, ethanol and carbon dioxide) in the as-spun $Y_3Al_5O_{12}$ -PVA composite nanofibers while the major weight loss was due to the combustion of organic PVA matrix. The plateau formed between 500 and $800\text{ }^\circ\text{C}$ on the TG curve indicated the formation of crystalline $Y_3Al_5O_{12}$ as the decomposition product [34, 35], as confirmed by FT-IR and XRD analyses shown in Figs. 6 and 7, respectively.

FTIR spectra of the $Y_3Al_5O_{12}/PVA$ composite nanofibers before and after calcination is shown in Fig. 6 (a and b). The Sample contains Al–O and Y–O bond along with some O–H implying presence of some hydroxyl group. Presence of O–H is not uncommon due to the presence of PVA. The as spun fiber mats exhibited Al–O stretching mode for octahedral co-ordination before calcination but when the sample was heat treated at $900\text{ }^\circ\text{C}$ Al–O stretching mode both for octahedral and tetrahedral co-ordination were noticed. From literature, [36], it was found that Al is hexa-coordinated in aqua complex and in Al_2O_3 , but in YAG, Al exhibited both tetra and hexa-coordination. On calcinations the tetrahedral Al cation normally changes to octahedral co-ordination. However in sol-gel technique, the cations polymerized into gel form maintaining its co-ordination partially in octahedral and partly in tetrahedral form. Therefore, on calcination, Fig. 6 (b), this $Y_3Al_5O_{12}/PVA$ composite nanofibers was converted to the pure $Y_3Al_5O_{12}$ containing Al in both tetrahedral and octahedral co-ordination as is in YAG. This was probably the reason of early bulk conversion of precursor nanofiber to YAG.

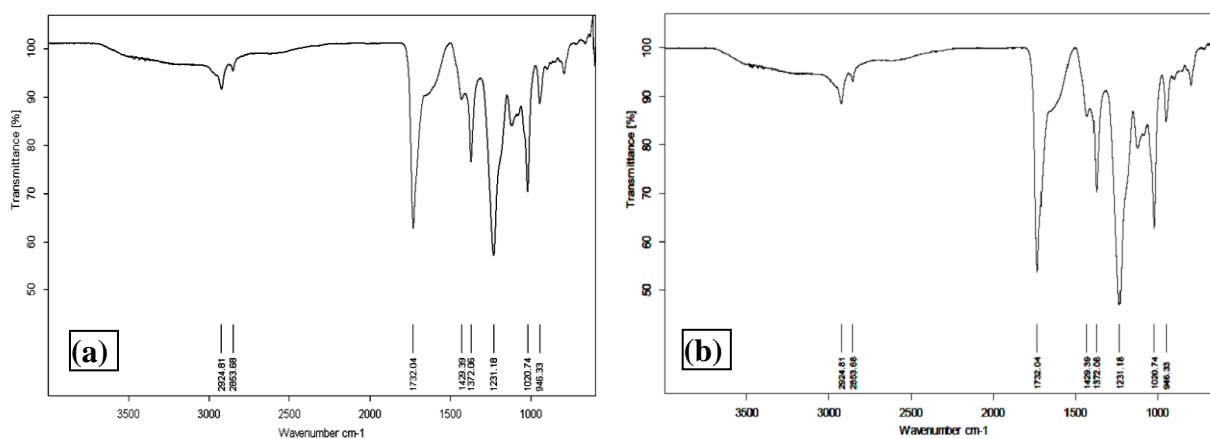


Figure 6. FT-IR spectra of the (a) $Y_3Al_5O_{12}/PVA$, (b) $Y_3Al_5O_{12}$ samples calcined in air for 2 h at $900\text{ }^\circ\text{C}$

The X-ray diffraction patterns of YAG nanofibers calcined at different temperatures are shown in Fig.7. It is clear that, the diffraction peaks of YAG calcined at $800\text{ }^\circ\text{C}$ can be indexed as crystalline YAG phase and no intermediate phases such as YAP and YAM can be detected. Further calcining of the nanofibers up to $900\text{ }^\circ\text{C}$ shows an increase of diffraction peak intensity and a decrease of diffraction peak full-width at half-maximum (FWHM) due to the improved crystallinity and grain

growth. High and sharp peaks are observed when the temperature is elevated to 1000 °C. The results of XRD above reveal that pre-calcination can lower the crystallization temperature of YAG phase comparing with the process without precalcination [38].

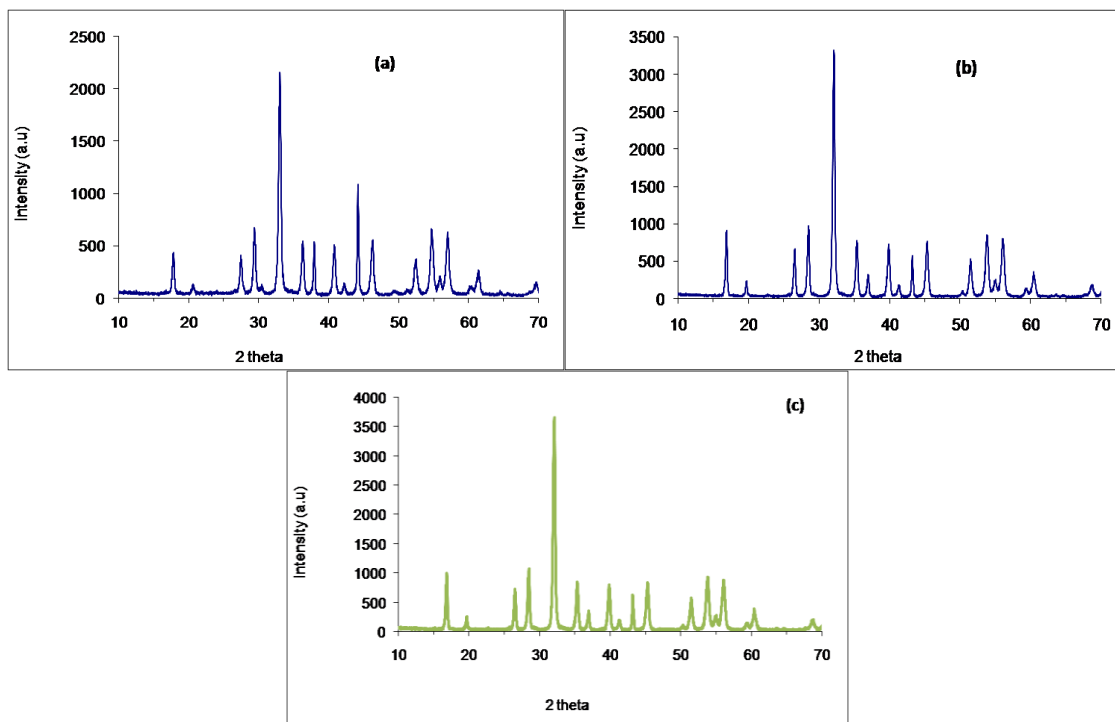


Figure 7. XRD patterns of YAG nanofibers calcined at different temperatures for 2 h (a) 800 °C (b) 900 °C (c) 1000 °C

SEM photographs of the aluminum yttrium oxide fibers obtained after calcinations at different temperatures were presented in Fig. 8. The PVA was selectively removed by calcination of the as spun composite nanofibers in air at 800, 900, and 1000 °C. From Fig. 8 (a) it is clearly seen that well-dispersed YAG nanofiber was synthesized by electrospinning followed by calcination process except for a few agglomerations of several particles. It can be noted that the sample calcined at 800 °C remained as continuous structures, Fig. 8 (a), and their diameters are somehow reduced. The reduction of nanofiber size of YAG calcined at 800 °C can be attributed to shrinkage resulted from burning of PVA. By contrast, nanofibers calcined at 900 and 1000 °C is filled with hard particle agglomerations as shown in Fig. 8 (b) and (c). After calcination at 900 and 1000 °C, the nature of nanofibers changed, and a structure of packed particles or crystallites was prominent, which may be due to the reorganization of the $Y_3Al_5O_{12}$ structure at high temperature. The morphology of the samples of $Y_3Al_5O_{12}$ nanofibers calcined at 900 and 1000 °C are converted into elongated and agglomerated nanoparticles. This result can be understood by considering that a polymer molecule adsorbed on the surface of a precursor has a higher decomposition temperature, and its continued existence at a relatively high temperature may reduce the diffusion of elements between particles that contribute to better dispersion of the powder. The changes in the morphology are related to a dramatic change in crystal structure as observed in electrospun $NaCO_2O_4$ [37] and $Ba_{0.6}Sr_{0.4}TiO_3$ [39].

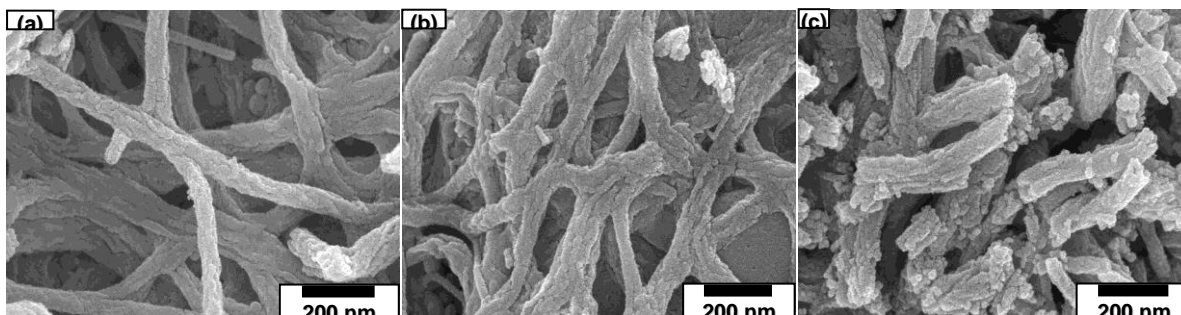


Figure 8. SEM morphologies of YAG nanofibers calcined at different temperatures for 2 h. (a) 800 °C, (b) 900 °C and (c) 1000 °C.

4. CONCLUSION

Nanostructures of $Y_3Al_5O_{12}$ have been successfully fabricated using an electrospinning technique. Polycrystalline $Y_3Al_5O_{12}$ nanofibers (diameter of ~60–200 nm) as confirmed by XRD were formed after calcination of the as-spun $Y_3Al_5O_{12}$ -PVA composite nanofibers in air at 800, 900 and 1000 °C for 2 h. The crystal structure and morphology of the nanofibers were influenced by the calcination temperature. We believe the electrospun $Y_3Al_5O_{12}$ nanofibers could have potential in many applications as nanocomposites, separation, anodic material in lithium ion batteries, catalysts, and as electronic material for nanodevices and storage devices.

ACKNOWLEDGEMENT

This work was financially supported by the National Plan for Science & Technology (NPST), King Saud University. Project No. 10-ADV1033-02

References

1. J. D. French, J. Zhao, M. P. Harmer, H. M. Chan, and G. A. Miller, *J. Am. Ceram. Soc.*, , 77, (1994) 2857–2865.
2. M. Veith, S. Mathur, A. Kareiva, M. Jilavi, M. Zimmer, and V. Huch, *J. Mater. Chem.*, 9, (1999) 3069–3079.
3. I. Shoji, S. Jurimura, Y. Sato, T. Taira, A. Ikesue, K. Yoshida, *Appl. Phys. Lett.* 77 (7) (2000) 939–941.
4. C. Park, S. Park, B. Yu, H. Bae, C. Kim, C. Pyun, G. Hong, *J. Mater. Sci. Lett.* 19 (2000) 335–338.
5. A. Ikesue, I. Furusato, K. Kamata, *J. Am. Ceram. Soc.* 78 (1) (1995) 225–228.
6. R. S. Hay, and L. E. Matson, *Acta Metall. Mater.*, 39, (1991) 1981–1994.
7. A. Towata, , H. J. Hwang, M. Yasuoka, and M., *J. Sando, Am. Ceram. Soc.*, 81, (1998) 2469–2472.
8. M. Schehl and R. Torrecillas, *Acta Mater.*, 50, (2002) 1125–1139.
9. W. Q. Li and L. Gao, *Nanostruct. Mater.*, 11, (1999) 1073–1080.
10. H. Wang and L. Gao, *Ceram. Int.*, 27, (2001) 721–723.
11. J. Li, Y.S.Wu, Y.B. Pan, W.B. Liu, L.P. Huang, J.K. Guo, *Opt. Mater.* 31 (2008) 6–17.

12. M.S. Tsai, W.C. Fu, W.C. Wu, C.H. Chen, C.H. Yang, *J. Alloys Compd.* 455 (2008) 461–464.
13. C.C. Chiang, M.S. Tsai, C.S. Hsiao, M.H. Hon, *J. Alloys Compd.* 416 (2006) 265–269.
14. H. Gong, D.Y. Tang, H. Huang, J. Ma, *J. Am. Ceram. Soc.* 92 (2009) 812–817.
15. Y.H. Zhou, J. Lin, M. Yu, S.M. Han, S.B. Wang, H.J. Zhang, *Mater. Res. Bull.* 38 (2003) 1289–1299.
16. Y. Hakuta, T. Haganuma, K. Sue, T. Adschiri, K. Arai, *Mater. Res. Bull.* 38 (2003) 1257–1265.
17. Z.H. Sun, D.R. Yuan, H.Q. Li, X.L. Duan, H.Q. Sun, Z.M. Wang, *J. Alloys Compd.* 379 (2004) L1–L3.
18. J.J. Zhang, J.W. Ning, X.J. Liu, Y.B. Pan, L.P. Huang, *Mater. Lett.* 57 (2003) 3077–3081.
19. Q.M. Lu, W.S. Dong, H.J. Wang, X.K. Wang, *J. Am. Ceram. Soc.* 85 (2002) 490–492.
20. H.M.H. Fadlalla, C.C. Tang, E.M. Elssfah, F. Shi, *Mater. Chem. Phys.* 109 (2008) 436–439.
21. C.H. Lu, W.T. Hsu, C.H. Hsu, H.C. Lu, B.M. Cheng, *J. Alloys Compd.* 456 (2008) 57–63.
22. T. Tachiwaki, M. Yoshinaka, K. Hirota, T. Ikegami, S. Yamaguchi, *Solid State Commun.* 119 (2001) 603–606.
23. Y.S. Ahn, M.H. Han, C.O. Kim, *J. Mater. Sci.* 31 (1996) 4233–4240.
24. J. Li, T. Ikegami, J. Lee, T. Mori, *J. Mater. Res.* 15 (7) (2000) 1514–1523.
25. M. A. Abu-Saied, Khalil Abdelrazek Khalil, Salem S. Al-Deyab, *Int. J. Electrochem. Sci.*, 7 (2012) 2019 - 2027.
26. El-Sayed M. Sherif, Mahir Es-saheb, Ahmed El-Zatahry , El-Refaie kenawyand and Ahmad S. Alkaraki, *Int. J. Electrochem. Sci.*, 7 (2012) 6154 - 6167
27. Mahir Es-saheb, Ahmed A. Elzatahry, El-Sayed M. Sherif , Ahmad S. Alkaraki , El-Refaie kenawy, *Int. J. Electrochem. Sci.*, 7 (2012) 5962 - 5976
28. Serge Rebouillat, Michael E.G. Lyons, *Int. J. Electrochem. Sci.*, 6 (2011) 5731 - 5740.
29. C. Shao, H. Guan, Y. Liu, J. Gong, N. Yu, X. Yang, *J. Crystal Growth* 267 (2004) 380.
30. P. Viswanathamurthi, N. Bhattarai, H.Y. Kim, D.R. Lee, *Nanotechnology* 15 (2004) 320.
31. S.J. Lee, C.H. Lee, W.M. Kriven, *J. Ceram. Process. Res.* 1 (2000) 92.
32. M. Harada, M. Goto, *J. Alloys Compds.* 408–412 (2006) 1193.
33. A. Thierauf, R. Jahn, S. Merklein, F. Essl, D. Sporn, M. Baier, A. Forchel, *Adv. Sci. Technol. 3D* (1995) 2717.
34. S. Nausing, S. Ninmuang, W. Jareernboon, S. Maensiri, S. Seraphin, *Mater. Sci. Eng. B* 131 (2006) 147.
35. S. Maensiri, W. Nuansing, J. Klinkaewnarong, P. Laokul, J. Khemprasit, *J. Colloid Interface Sci.* 297 (2006) 578.
36. I. Warshaw, R. Ray, *J. Am. Ceram. Soc.* 42 (1959) 434–438.
37. S. Maensiri, W. Nuansing, *Mater. Chem. Phys.* 99 (2006) 104.
38. L. Yang, T. Lu, H. Xu, N. Wei, *Journal of Alloys and Compounds* 484 (2009) 449–451
39. S. Maensiri, W. Nuansing, J. Klinkaewnarong, P. Laokul, J. Khemprasit, *J. Colloid Interface Sci.* 297 (2006) 578.